Dependence of photocatalytic activity on particle size of a shape-controlled anatase titanium(IV) oxide nanocrystal

Dependence of photocatalytic activity on particle size of a shape-controlled anatase titanium(IV) oxide nanocrystal

Naoya Murakami[a], Shota Kawakami[a] Toshiki Tsubota[a] and Teruhisa Ohno[a,b,*]

[a]Department of Applied Chemistry, Faculty of Engineering, Kyushu Institute of Technology, 1-1 Sensuicho, Tobata, Kitakyushu 804-8550, Japan

[b]JST, PRESTO, 4-1-8 Honcho Kawaguchi, Saitama 332-0012, Japan

* Corresponding author. TEL/FAX: +81-93-884-3318

E-mail address: tohno@che.kyutech.ac.jp (T. Ohno)

Keywords: Photocatalyst; titanium(IV) oxide; decahedral anatase; separation of redox sites; acetaldehyde decomposition.

Abstract

Decahedral anatase titanium(IV) oxide (TiO_2) with {101} and {001} exposed crystal faces was prepared by hydrothermal treatment of peroxo titanic acid (PTA) solution with polyvinyl alcohol (PVA) as a shape-control reagent. pH of the PTA solution and amounts of PVA and amorphous titania included in the PTA solution had a large influence on size and shape of the prepared particles, and particle width of the decahedral anatase TiO_2 was controllable between 25 and 60 nm. Photocatalytic activity of the decahedral anatase TiO_2 was examined in terms of the relationship between particle size and photocatalytic activity. Decahedral anatase TiO_2 with particle width of ca. 40 nm showed excellent activity because of the optimized balance between efficient separation of redox sites and large specific surface area.

1. Introduction

Crystal size is one of the most important properties influencing performance of material function. Nano-sized particles have been expected to exhibit excellent performance due to their large specific surface area and quantum size effect. For example, nano-sized particles having a large numbers of adsorption sites have frequently been used in photocatalytic reaction, which has been a promising function for environmental remediation [1,2]. Photocatalytic reaction is induced by excited electrons and positive holes, followed by reduction and oxidation with surface-adsorbed species. However, back reaction easily occurs on the nanoparticle surface because reduction and oxidation proceeds in neighboring sites, and this back reaction as well as recombination between excited electrons and positive holes greatly decrease the efficiency of photocatalytic reaction. Therefore, it is important to optimize the balance between adsorption ability and utilization efficiency of photogenerated electrons and positive holes by enlargement of the specific surface area, an improvement of crystallinity by thermal treatment and combined use with other materials.

Recently, the dependence of photocatalytic activity on exposed crystal faces of an anatase titanium(IV) oxide (TiO_2) nanocrystal has been intensively studied [3-10]. Our group has also proposed that anatase TiO_2 with specific exposed crystal faces exhibits higher photocatalytic activity because of spatial separation of redox sites induced by different kinds of exposed crystal faces [11,12]. In our previous study, we prepared decahedral anatase TiO_2 particles with {101} and {001} exposed crystal faces by hydrothermal treatment of peroxo titanic acid (PTA) with polyvinyl alcohol (PVA) as a shape-control reagent [12]. PTA species are known as a water-base precursor for TiO_2 with relatively high stability against hydrolysis over a wide pH range under ambient condition [13]. Moreover, shape-control reagent, such as organic acid and hydrophilic polymer, easily coordinate on the peroxio titanic acid species [12,14]. These properties are suitable for formation of specific exposed crystal faces. The prepared anatase TiO_2 prepared in previous study showed higher activity than that of P-25, which is a well-known commercial TiO_2 [12]. This is presumably because of separation of redox sites induced by predominant reduction and oxidation over {101} and {001} exposed crystal faces, which were determined by

photodeposition method [11,12]. However, the prepared shape-controlled anatase TiO_2 had a primary particle size of ca. 25 nm, which is thought to be insufficient for efficient separation of redox sites. Thus, an increase in the particle size of a shape-controlled nanocrystal will possibly enhance photocatalytic activity as a result of more effective separation of redox sites (Figure 1).

Here, we report a method for preparation of a decahedral anatase TiO_2 nanocrystal with larger particle size than that of TiO_2 prepared in our previous study [12]. Precursor conditions, i.e., pH of the PTA solution (pH_{PTA}) and amounts of PVA (M_{PVA}) and amorphous titania (M_{am}) included in the PTA solution, had a large influence on size and shape of the prepared particles. Moreover, stirring during hydrothermal treatment was carried out for improvement of particle size distribution and surface structure. In the present study, photocatalytic activity of the prepared shape-controlled anatase TiO_2 was examined in terms of the relationship between particle size and photocatalytic activity.

2. Experimental Section

2.1. Sample Preparation

Milli-Q water (3.0 cm^3) was added to 10 cm^3 of titanium(IV) ethoxide and 50 cm^3 of ethanol with vigorous stirring, and the mixture was stirred for 1 h at room temperature. The resulting precipitate was centrifugally separated from the solution and dried under reduced pressure. One or three milligrams of obtained amorphous titania was dispersed in 100 cm^3 of milli-Q water and then irradiated by ultrasonication. 32 cm^3 of 30% hydrogen peroxide was added, and yellow peroxo titanic acid (PTA) solution was obtained. After 3 h, pH of the solution was adjusted to 7 by adding ammonium (NH_3) solution, and a certain amount of polyvinyl alcohol (PVA, M_W = 22,000) as a shape-control reagent was added to the solution. Excess amount of solution was evaporated by stirring the solution at ca. 60 °C, and then the solution was cooled down. Finally, pH and volume of the solution were adjusted to 7, 9, 10 or 11 and to 70 cm^3, respectively, by addition of NH_3 solution.

The solution in a Teflon bottle sealed with a stainless jacket (Sanaikagaku Co., HU-100) was

heated at 200 °C for 48 h in an oven. Hydrothermal treatment with magnetic stirring was carried out using a hydrothermal reactor with a magnetic stirrer (Sanaikagaku Co., RDV-TMS-100 and HM-19G-U). After hydrothermal treatment, the residue in the Teflon bottle was washed with milli-Q water until ionic conductivity of the supernatant was <10 μS cm^{-2}. The particles were dried under reduced pressure at 60 °C for 12 h. The obtained powders were thermally treated at 350 ^{o}C for 2 h in order to remove residual organic compounds on the TiO_2 particles.

2.2. Characterization

The crystal structures of the TiO_2 powders were characterized with an X-ray diffractometer (Rigaku, MiniFlex II) with Cu Kα radiation (λ = 1.5405 Å). Primary particle size for the prepared samples (d_{hkl}) were estimated from peaks attributed to anatase hkl in XRD patterns using the Scherrer equation:

$$d_{hkl} = 0.9\lambda/\beta_{hkl}\cos\theta_{B,hkl},$$

where λ is the wavelength of X-rays, $\theta_{B,hkl}$ is the Bragg angle and β_{hkl} is the full width at half maximum corrected by the full width at half maximum of silicon powders. The specific surface areas (S_{BET}) of the particles were determined with a surface area analyzer (Quantachrome, Nova 4200e) by using the Brunauer-Emmett-Teller equation. The morphology of prepared TiO_2 particles was observed by using scanning electron microscopy (SEM; JEOL, JSM-6701FONO). Average particles of width (W_{ave}), length (L_{ave}) and aspect ratio (r_{asp}) were estimated by SEM observation. The crystal size values of W_{ave} and L_{ave} showed linear relationship with d_{101} and d_{200}, and d_{004}, which were determined by the XRD peaks using Scherrer equation. Due to the difficulty in estimation of particle size by SEM observation, average particle sizes for AMT-100 (TAYCA Co.) and ST-01 (Ishihara Sangyo Co.) were estimated to be 6 nm and 8 nm from peaks attributed to anatase 101 in XRD patterns using the Scherrer equation.

2.3. Photocatalytic Decomposition of Acetaldehyde

Photocatalytic activities of TiO_2 samples were evaluated by photocatalytic decomposition of

acetaldehyde (AcH). Two hundred milligrams of TiO_2 powders, which have complete extinction of the incident radiation, were spread on a glass dish, and the glass dish (8.55 cm^2) was placed in a 125 cm^3 Tedlar bag (As one). Five hundred parts per million of gaseous AcH was injected into the Tedlar bag, and photoirradiation was performed at room temperature after the AcH had reached adsorption equilibrium. The gaseous composition in the Tedlar bag was 79% N_2, 21% O_2, < 0.1 ppm of CO_2 and 500 ppm of acetaldehyde, and relative humidity was ca. 30%. A light-emitting diode (Nichia, NCCU033), which emitted light at a wavelength of ca. 365 nm and an intensity of 100 μW cm^{-2}, was used as the light source. The light intensity was measured by an optical power meter (HIOKI, 3664). The concentrations of AcH and carbon dioxide (CO_2) were estimated by gas chromatography (Agilent Technologies 3000, micro TCD detector) with PLOT-Q and OV1 columns. AMT-100, AMT-600, TKP-102, TITANIX JA-1 (TAYCA Co.) and ST-01, ST-21 and ST-41 (Ishihara Sangyo Co.) as commercial anatase TiO_2 powders and P-25 (Japan Aerosil Co.) as a standard TiO_2 powder were used.

3. Results and Discussion

All of the prepared samples were attributed to single-phase anatase TiO_2 structure from results of XRD analysis. This coincided with results of our previous study indicating that hydrothermal treatment of PTA solution under a high pH_{PTA} condition induced preferential formation of anatase TiO_2 structure [12]. However, primary particle size and shape of the prepared TiO_2 strongly depended on pH_{PTA} and M_{PVA}. Figure 2 shows SEM images and histograms of widths and lengths of the particles obtained from SEM observation of representative prepared samples. TiO_2 prepared in most conditions showed a decahedral shape with large {101} and small {001} exposed crystal faces, judging from angles between exposed crystal faces in SEM images. This shape was similar to that of TiO_2 prepared by hydrothermal treatment of PTA solution at pH 7, which showed particle width of ca. 25 nm (Fig. 2(a,e)) [12]. However, anatase TiO_2 particles prepared by hydrothermal treatment of PTA solution with a lower ratio of M_{PVA} to M_{am} under a higher pH_{PTA} condition had widths of more than 30 nm (Fig. 2(b,f), (c,g), (d,h)). Addition of a small amount of PVA (10 mg

of PVA) under a high pH_{PTA} condition induced rod-like growth (Fig. 3 (a,c)), similar to that of the sample prepared without PVA addition (Fig. 3 (b,d)). Side faces of the rod were presumably attributed to {100} faces or zigzag surface of {101} faces [12]. Similar anatase rods were prepared by PTA solution and aqueous solution of sodium hydroxide in other studies [15,16]. These results indicate that PVA in PTA solution induces formation of {101} exposed crystal faces and retardation of growth in the [001] direction, which was promoted under a high pH condition. Some reports suggests that alcohol show more strongly adsorption to the {001} faces, which depressed the growth rate along the [001] direction [17]. Thus, PVA is thought to act in a similar way.

On the other hand, a larger amount of PVA induced a narrower distribution of particle widths and lengths though increase of particle width and length was retarded to some extent. These results indicate that PVA works not only as a regulator of crystal growth in the [001] direction but also as a separator for prevention of particle aggregation in a hydrothermal growth process. Therefore, formation of well-defined faces requires appropriate M_{PVA} and pH_{PTA}. Although higher pH_{PTA} increased particle size up to ca. 80 nm (Fig. 2 (d,h)), the shapes and sizes of particles were not uniform. This is because rapid hydrolysis of PTA to titania under a high pH condition presumably induced formation of non-uniform particles having no well-defined faces and a wide distribution of sizes.

Figure 4 shows SEM images and histograms of particle width and length obtained from SEM observation of TiO_2 prepared by hydrothermal treatment with magnetic stirring. Stirring during the hydrothermal treatment did not induce a change in crystal structure but induced a decrease in particle size distribution. This was clearly observed in TiO_2 prepared under a high pH_{PTA} condition and large M_{PVA}, and surface structure, i.e., well-defined exposed crystal faces, was improved.

Photocatalytic activity was evaluated by decomposition of acetaldehyde under ultraviolet irradiation. Figure 5 shows photocatalytic activity as an initial rate of carbon dioxide (CO_2) generation against particle widths of commercial and prepared anatase TiO_2 samples.

Photocatalytic activity for commercial anatase TiO_2 samples showed a monotonic increase with increase in particle size and saturation tendency with particle width of more than 40 nm. This result can be explained by a trade-off relationship between particle size (crystallinity) and specific surface area (adsorption sites), though photocatalytic activity depends also on other physical and chemical properties. Higher photocatalytic activity for decahedral anatase with particle width of ca. 25 nm than that for commercial anatase indicates that two kinds of exposed crystal faces, i.e., {101} and {001} exposed crystal faces, induced efficient photocatalytic reaction as a result of separation of redox sites.

Photocatalytic activity of decahedral anatase TiO_2 increased with increase in particle width up to ca. 40 nm. This is because redox reaction proceeded more efficiently due to longer spatial separation of redox sites on larger particles. Electron diffusion length of more than a few micrometers in a polycrystalline anatase TiO_2 film [18] indicates that electrons generated near oxidation sites ({001} exposed crystal faces) can sufficiently migrate to reduction sites ({101} exposed crystal faces) in an anatase TiO_2 nanocrystal with particle size of ca. 40 nm.

In contrast, rod-like anatase TiO_2 prepared by hydrothermal treatment of PTA solution with less M_{PVA} showed lower activity with increase in particle width. This might be due to lower reduction performance of side-exposed crystal faces ({100} faces or zigzag surfaces of {101} faces). However, our group and other groups have shown that anatase TiO_2 with {100} faces or zigzag faces of {101} faces and moderate {001} faces shows sufficiently high photocatalytic activity [8,12, 16]. Therefore, the lower photocatalytic activity of rod-like anatase TiO_2 is attributable to not-optimized surface area ratio of reduction to oxidation sites [19].

Further increase in particle size (> ca. 40 nm) of decahedral anatase deteriorated photocatalytic activity because of the decrease in specific surface area as well as worse-defined faces, resulting in less efficient separation of redox sites. Actually, anatase TiO_2 prepared under the condition of large M_{PVA} and high pH_{PTA} with stirring showed a higher photocatalytic activity than that of anatase TiO_2 prepared without stirring because stirring during the hydrothermal growth process improved

surface structure (Fig. 2(b,f) → Fig. 4(a,e), Fig. 2(c,g) → Fig. 4(c,g), Fig. 2(d,h) → Fig. 4(d,h)). However, even among anatase TiO_2 samples with well-defined faces, photocatalytic activity decreased with increase in particle size from 40 nm to 60 nm. These results also indicate that well-defined faces as well as specific surface area are important factors for higher photocatalytic activity. Difference in surface area ratio of {001} to {101} for decahedral anatase TiO_2 might have an influence on efficiency of photocatalytic reaction. However, slight differences in the aspect ratio evaluated from SEM observation (1.35~1.46) and the integrated intensity ratio of anatase 004 peak to that of anatase 101 peak in XRD patterns (0.185~0.220) for decahedral anatase TiO_2 indicate that the difference in surface area ratio of {001} to {101} was not large enough to change the photocatalytic efficiency.

4. Conclusions

In this paper, we discussed the relationship between photocatalytic activity and particle size of decahedral anatase TiO_2 with {101} and {001} exposed crystal faces. Anatase TiO_2 with well-defined faces showed higher activity, and decahedral anatase with particle width of ca. 40 nm showed excellent activity because of the optimized balance between efficient separation of redox sites and large specific surface area. The results of present study indicate that change in particle size as well as change in surface area ratio of reduction to oxidation sites of a shape-controlled nanocrystal has the potential to control reaction properties.

Acknowledgements

This work was supported by the Knowledge Cluster Initiative, Grant-in-Aid of Young Scientist (B) (22750139) implemented by the Ministry of Education, Culture, Sports, Science and Technology (MEXT), and the JST PRESTO program.

References

[1] M. R. Hoffmann, S. T. Martin, W. Choi and D. W. Bahnemann, Chem. Rev., 95 (1995) 69-96.

[2] A. Fujishima, T. N. Rao and D. A. Tryk, J. Photochem. Photobiol. C: Photochem. Reviews, 1 (2000) 1-21.

[3] F. Amano, T. Yasumoto, O. O. P. Mahaney, S. Uchida, T. Shibayama and B. Ohtani, Chem. Comm., (2009) 2311-2313.

[4] F. Amano, O. O. P. Mahaney, Y. Terada, T. Yasumoto, T. Shibayama and B. Ohtani, Chem. Mater., 21 (2009) 2601-2603.

[5] D. Zhang, G. Li, H. Wang, K. M. Chan and J. C. Yu, Crystal Growth & Design, 10 (2010) 1130-1137.

[6] F. Amano, T. Yasumoto, O. O. P. Mahaney, S. Uchida and T. Shibayama, Top. Catal., 53 (2010) 455-461.

[7] W. Q. Fang, X. Gong and H. G. Yang, J. Phys. Chem. Lett., 2 (2011) 725-734.

[8] J. Pan, G. Liu, G. Q. Lu and H. Cheng, Angew. Chem. Int. Ed., 50 (2011) 2133-2137.

[9] J. Li, Y. Yu, Q. Chen, J. Li and D. Xu, Cryst. Growth Des., 10 (2010) 2111-2115.

[10] T. Tachikawa, S. Yamashita and T. Majima, J. Am. Chem. Soc., 133 (2011) 7197-7204.

[11] T. Ohno, K. Sarukawa and M. Matsumura, New. J. Chem., 26 (2002) 1167-1170.

[12] N. Murakami, Y. Kurihara, T. Tsubota and T. Ohno, J. Phys. Chem. C, 113 (2009) 3062-3069.

[13] M. Kakihana, M. Tada, M. Shiro, V. Petrykin, M. Osada and Y. Nakamura, Inorg. Chem., 40 (2001) 891-894.

[14] K. Tomita, V. Petrykin, M. Kobayashi, M. Shiro, M. Yoshimura and M. Kakihana, Angew. Chem. Int. Ed. 45 (2006) 2378-2381.

[15] Y. Gao, H. Luo, S. Mizusugi and M. Nagai, Crystal Growth & Design, 8 (2008) 1804-1807.

[16] J. Li and D. Xu, Chem. Commun., 46 (2010) 2301-2303.

[17] J. H. Liao, L. Y. Shi, S. Yuan, Y. Zhao and J. H. Fang, J. Phys. Chem. C., 113 (2009) 18778–18783.

[18] S. Nakade, M. Matsuda, S. Kambe, Y. Saito, T. Kitamura, T. Sakata, Y. Wada, H. Mori and S.

Yanagida, J. Phys. Chem. B, 106 (2002) 10004-10010.

[19] N. Murakami, S. Katayama, M. Nakamura, T. Tsubota and T. Ohno, J. Phys. Chem. C, 115 (2011) 419-424.

Table 1. Summary of the preparation condition and average width (W_{ave}), average length (L_{ave}), aspect ratio (r_{asp}) and specific surface area (S_{BET}) of prepared samples.

sample	M_{am}/g	M_{PVA}/mg	pH_{PTA}	stirring	W_{ave}/nm	L_{ave}/nm	r_{ave}/nm	S_{BET}/m^2 g^{-1}
a	3	10	9	no	57.8	84.9	1.45	32
b	3	10	10	no	46.6	82.6	1.75	26
c	3	10	11	no	34.4	55.7	1.68	37
d	3	20	9	no	38.2	51.9	1.35	34
e	3	20	10	no	40.6	57.6	1.42	31
f	3	20	11	no	59.0	87.2	1.46	14
g	3	30	9	no	36.2	50.0	1.37	35
h	3	30	10	no	27.7	38.8	1.40	48
i	3	30	11	no	76.3	107.1	1.41	18
j	3	20	10	yes	44.1	60.7	1.36	35
k	3	20	11	yes	62.6	88.6	1.41	21
l	3	30	11	yes	60.2	83.4	1.39	23
m	3	25	10	yes	54.3	79.1	1.45	23
n	1	30	7	no	26.2	33.8	1.29	–
o	3	0	10	no	42.9	68.5	1.56	–

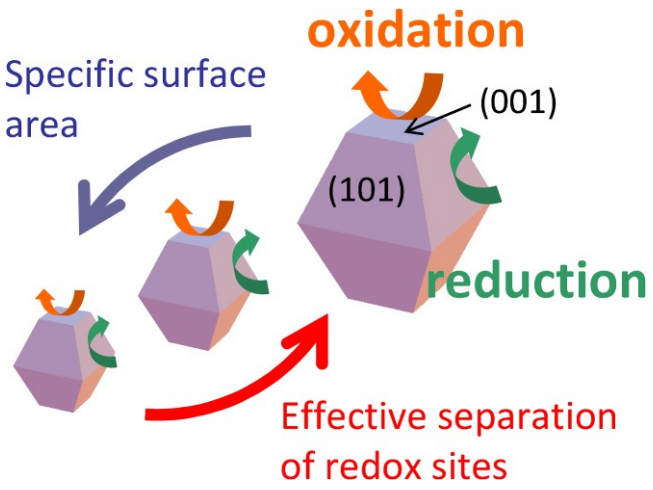

Figure 1. Caption Schematic image of photocatalytic reaction over octahedral anatase with different particle sizes.

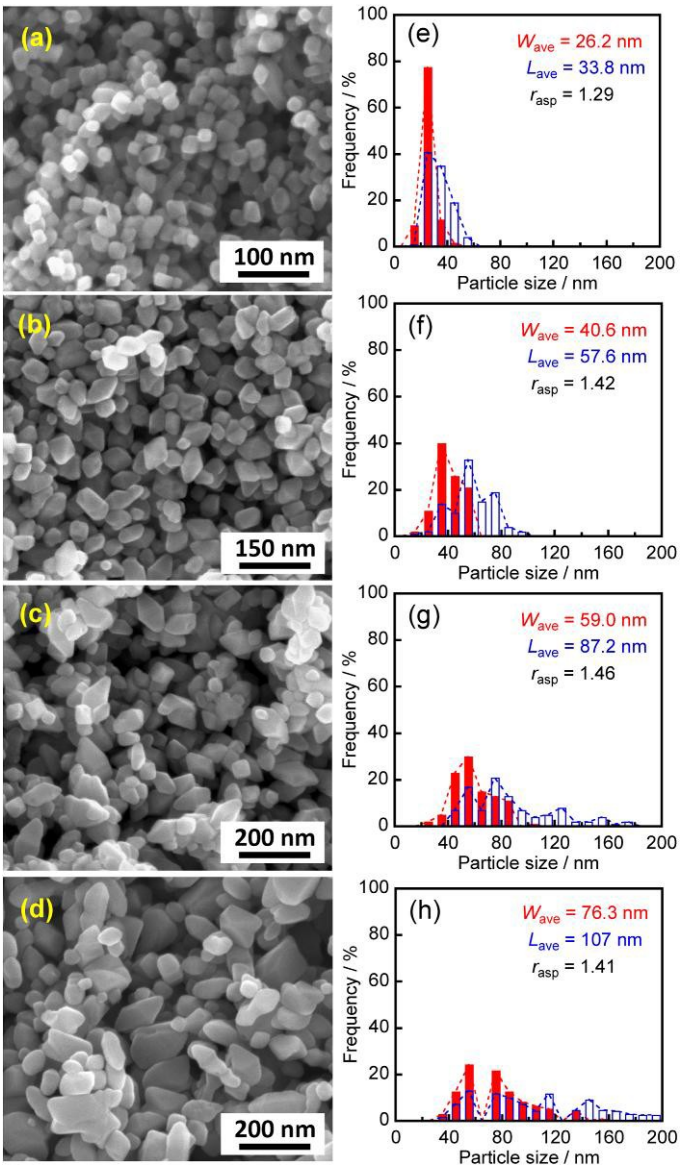

Figure 2. SEM images and histograms of particle width (red) and length (blue) obtained from SEM observation of the prepared anatase TiO_2. (a,e) sample-n, (b,f) sample-e, (c,g) sample-f and (d,h) sample-i.

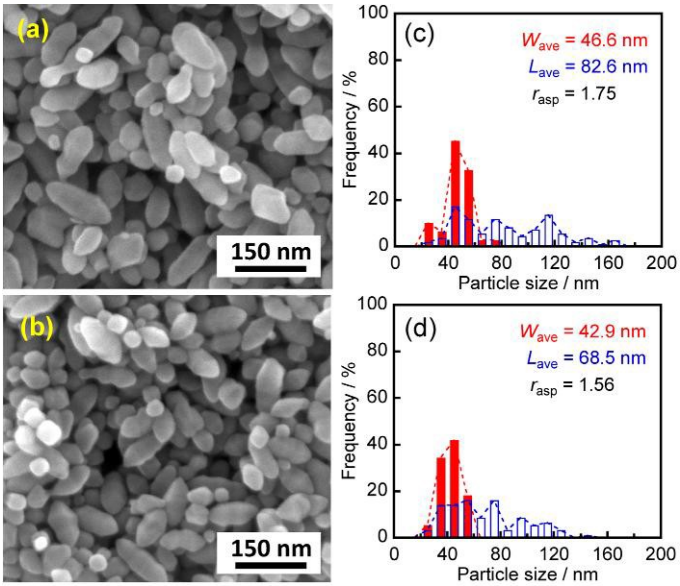

Figure 3. SEM images and histograms of particle width (red) and length (blue) obtained from SEM observation of the prepared anatase TiO_2. (a,c) sample-b and (b,d) sample-o.

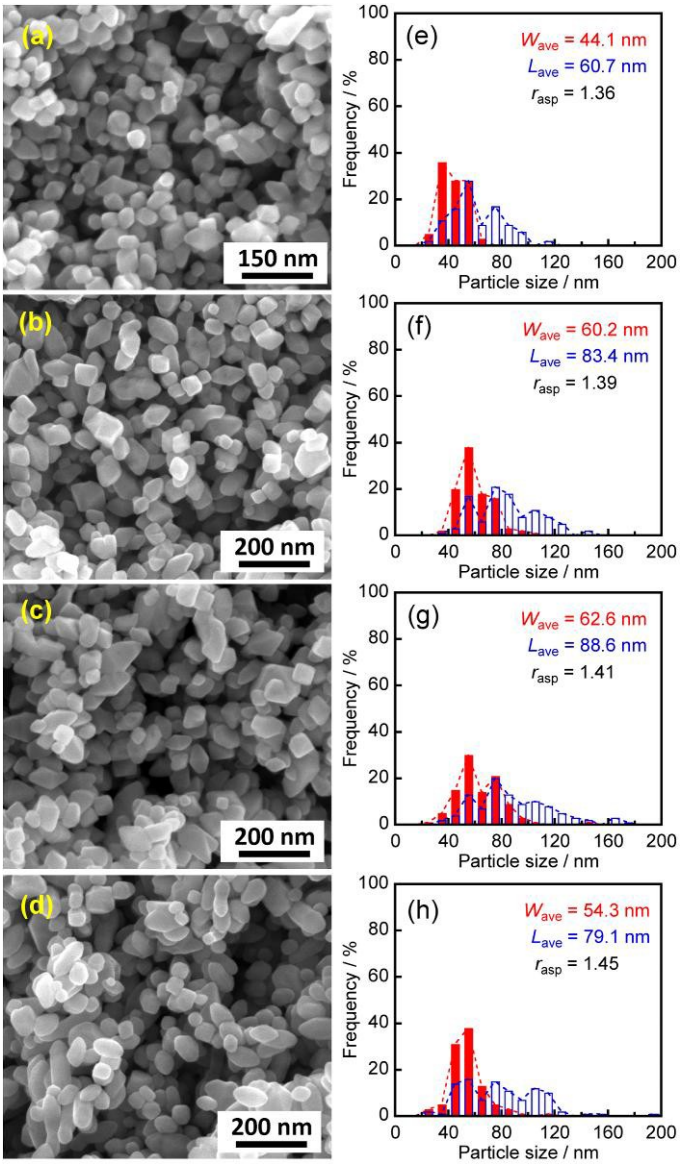

Figure 4. SEM images and histograms of particle width (red) and length (blue) obtained from SEM observation of the prepared anatase TiO_2 under the condition of stirring during hydrothermal treatment. (a,e) sample-j, (b,f) sample-m, (c,g) sample-k and (d,h) sample-l.

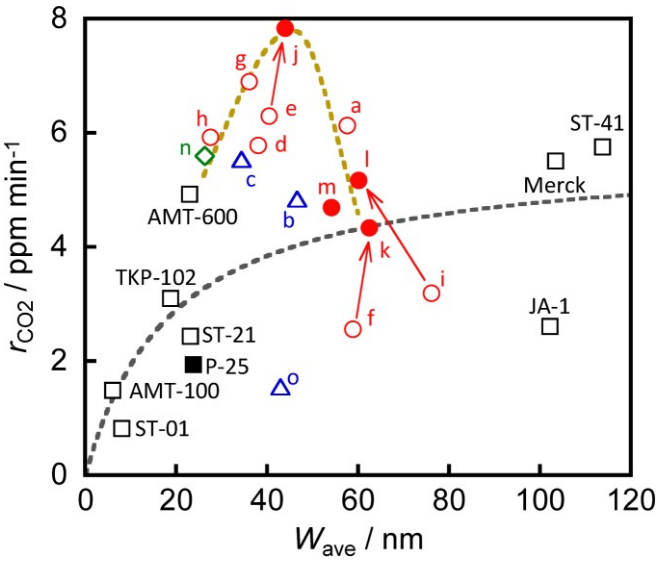

Figure 5. Initial rates of CO_2 generation as photocatalytic activity (k_{CO2}) against W_{ave} of (square) commercial TiO_2, (blue open-triangle) particles with r_{asp} of more than 1.5, (red open-circle) particles with r_{asp} of less than 1.5, (red filled-circle) samples prepared with stirring, (green open-diamond) sample-n.

Figure1
Click here to download high resolution image

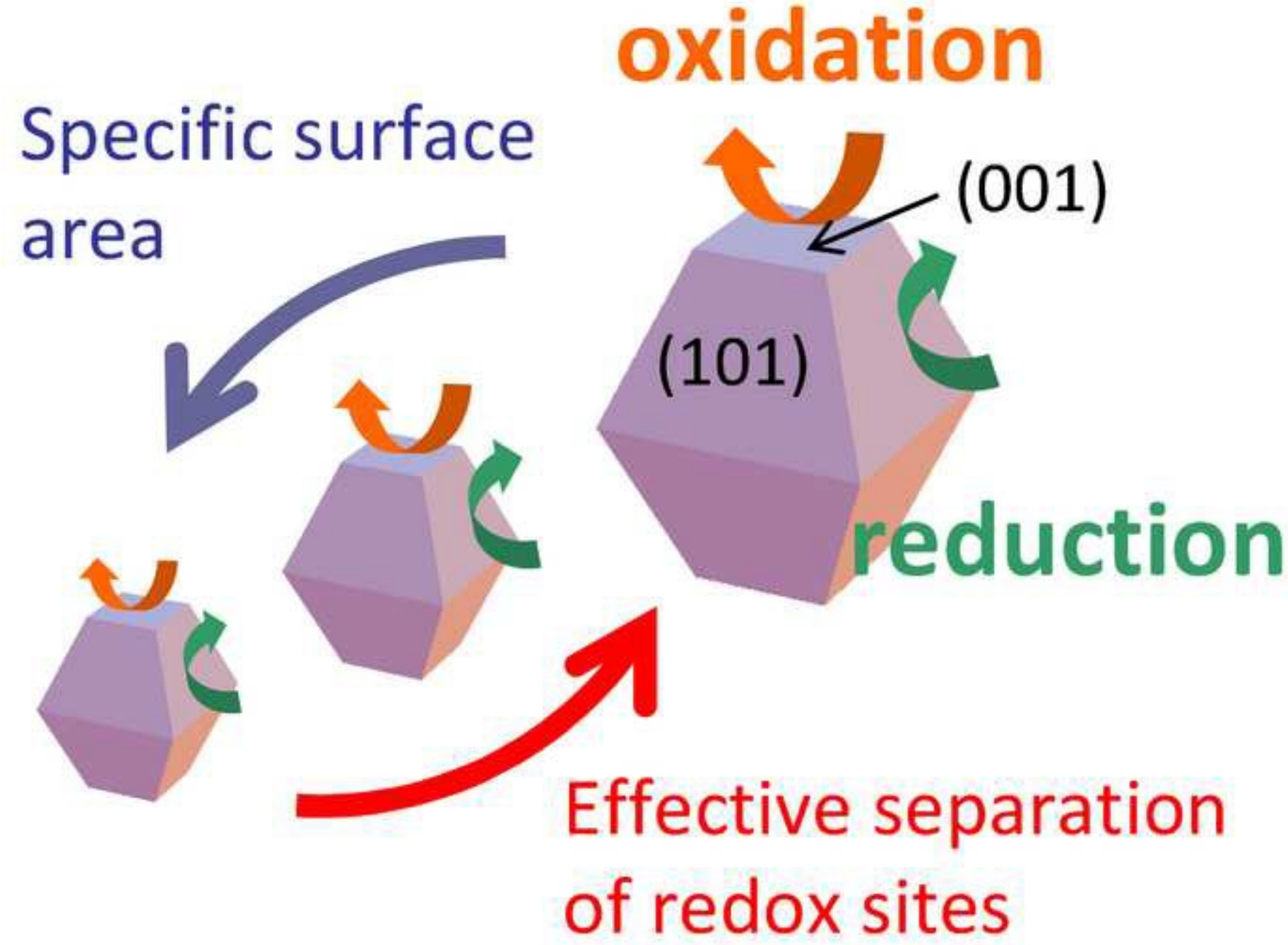

Figure2

Click here to download high resolution image

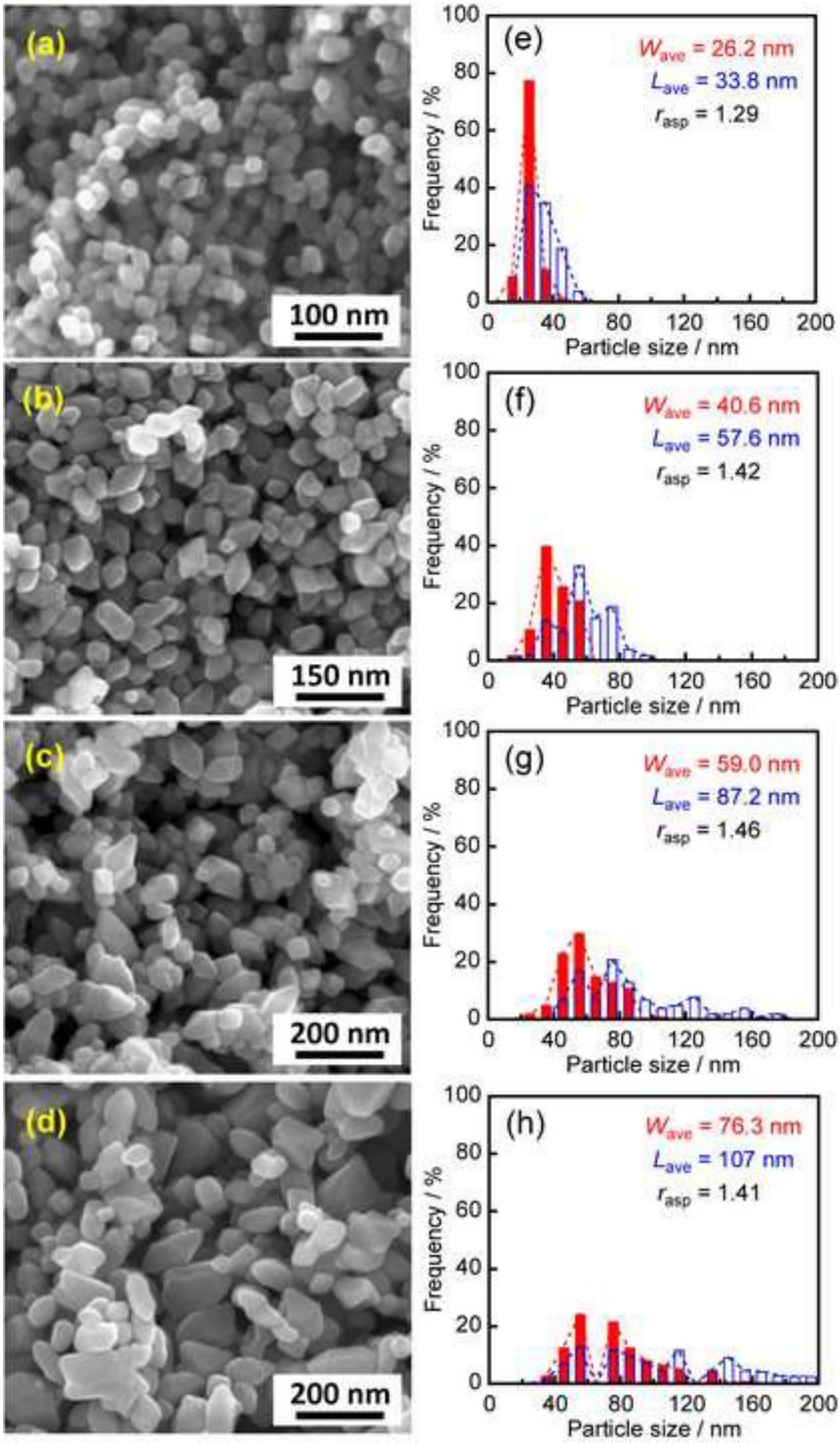

Figure3

Click here to download high resolution image

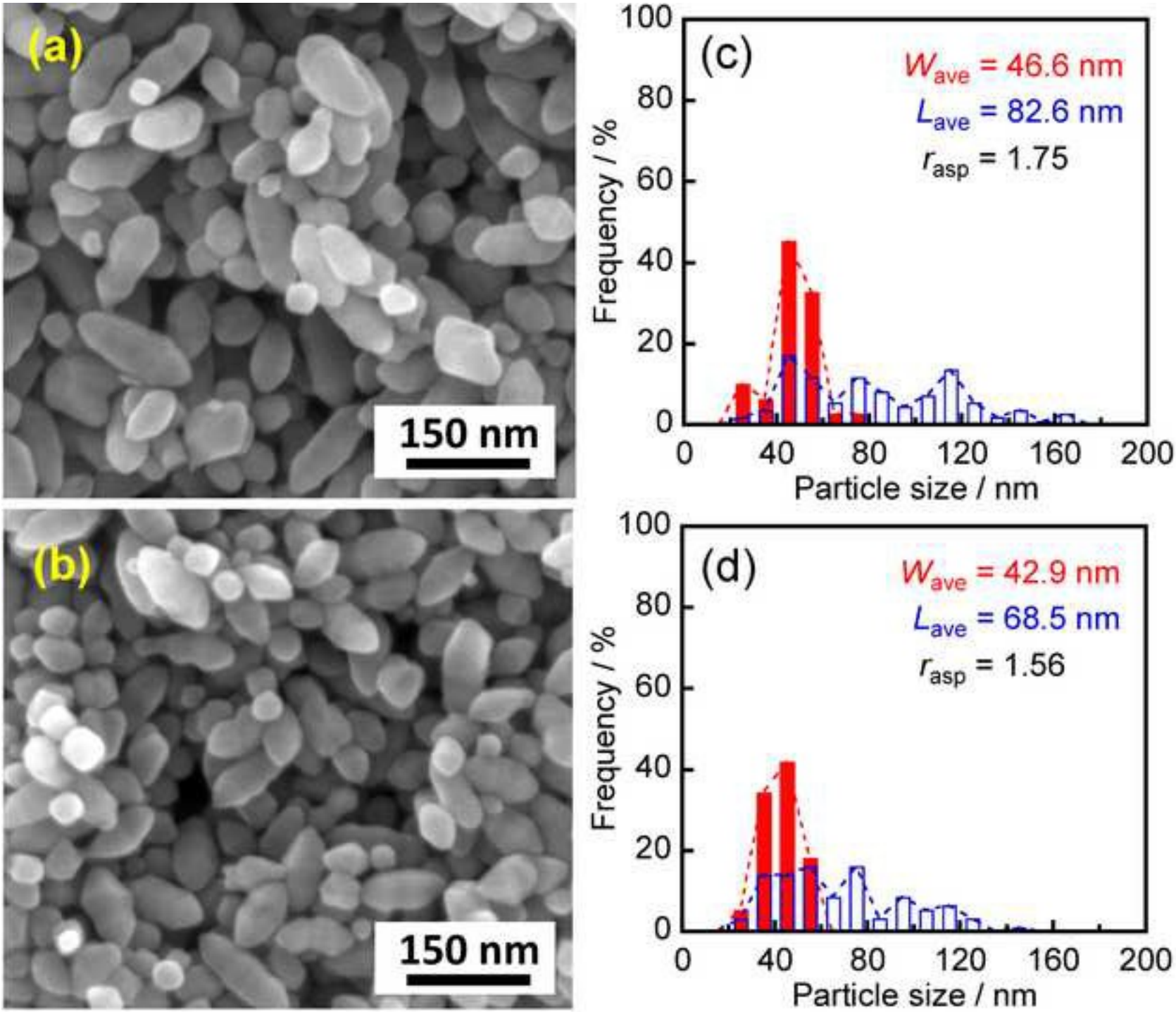

Figure4

Click here to download high resolution image

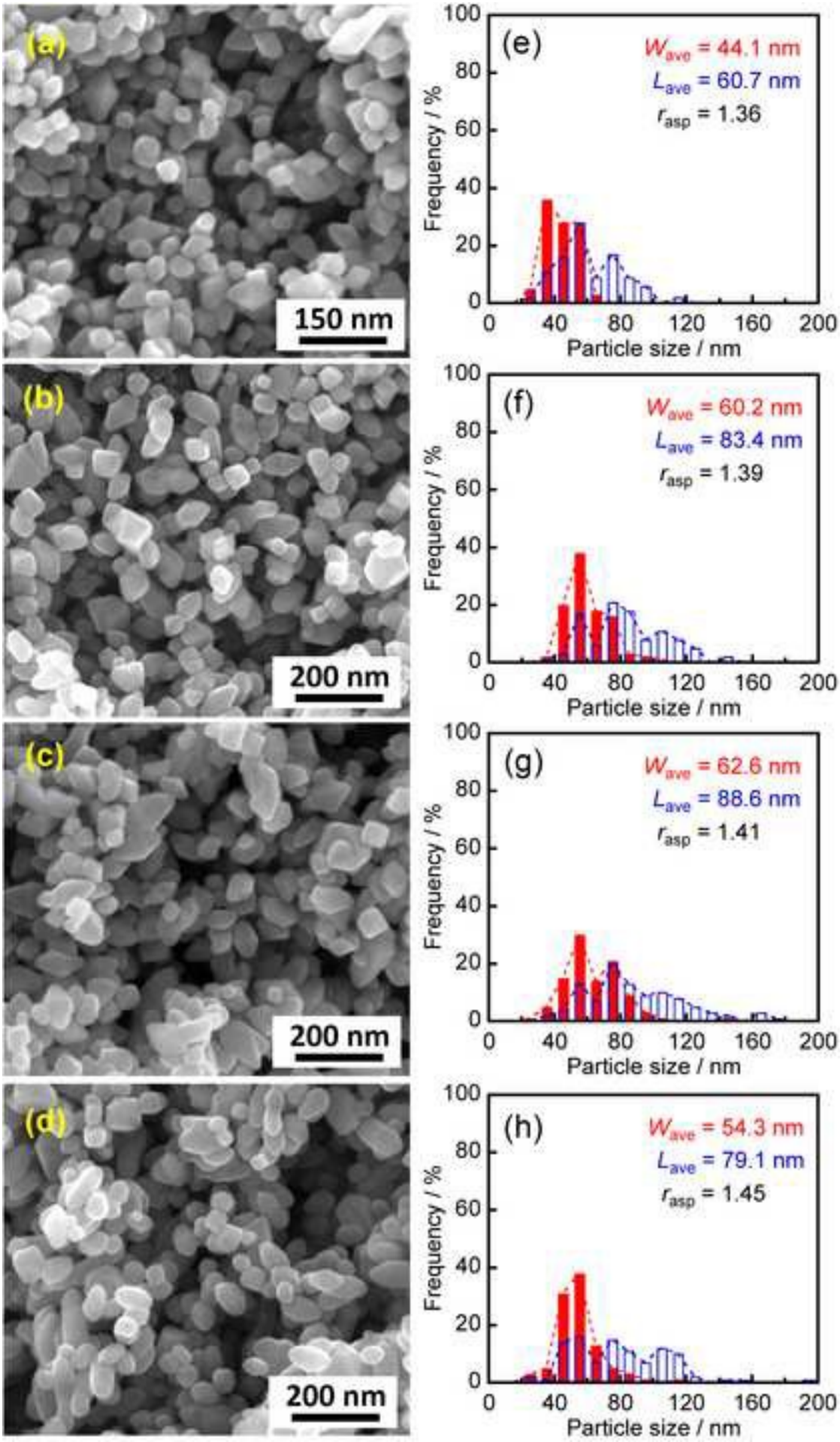

Figure5
Click here to download high resolution image